

The Relationship between Solution Structure and Crystal Nucleation: A Neutron Scattering Study of Supersaturated Methanolic Solutions of Benzoic Acid

R. C. Burton,[†] E. S. Ferrari,[†] R. J. Davey,^{*,†} J. L. Finney,[‡] and D. T. Bowron[§]

Molecular Materials Centre, School of Chemical Engineering & Analytical Science, The University of Manchester, P.O. Box 88, Manchester M60 1QD, U.K., Department of Physics & Astronomy and London Centre for Nanotechnology, University College London, Gower Street, London WC1E 6BT, U.K., and ISIS Facility, STFC, Rutherford Appleton Laboratory, Chilton, Didcot, Oxon, OX11 0QX, U.K.

Received: April 6, 2010; Revised Manuscript Received: June 2, 2010

In this contribution, neutron scattering experiments (with isotopic substitution) of concentrated and supersaturated methanolic benzoic acid solutions combined with empirical potential structure refinement (EPSR) were used to investigate the time-averaged atomistic details of this system. Through the determination of radial distribution functions, quantitative details emerge of the solution coordination, its relationship to the nature of the crystalline phase, and the response of the solution to imposed supersaturation.

Background

Crystallization from solution, an important process in the separation and purification of a wide range of inorganic and molecular materials,¹ utilizes nucleation as its key step. Molecules in a supersaturated solution are thought to undergo a process of self-assembly and clustering to yield a nucleus that may grow into a crystal. The metastability of supersaturated solutions results from the difficulty associated with creating an interface between solution and nuclei, particularly at low supersaturations.¹ The kinetics of this transition from solution to crystal have been successfully described using models first derived by Volmer and Becker and Doering.²

Increased availability of crystal structure information (e.g., via the Cambridge Structural Database³) has culminated in a view of a crystal as a supramolecular assembly with the process of nucleation often thought of as the first stage in the assembly process.⁴ Currently, there is significant interest in exploring the structural aspects of this process and in considering links between solution and crystal chemistry. Spitaleri et al.⁵ for example, have used complexation induced proton chemical shift measurements to model and visualize solution dimers so as to compare them with dimers present in the related crystal structures. Davey et al.,⁶ Chiarella et al.,⁷ and Chadwick et al.⁸ have used a combination of NMR and FTIR spectroscopy to study concentrated solutions of inosine, benzoic, tetrolic, and mandelic acids and the cocrystallizing system benzophenone-diphenylamine. Previous neutron scattering studies have been reported by Burton et al.^{9,10} for aqueous solutions of both urea and hexamethylene tetramine, which provided atomistic level data on both concentrated and supersaturated solutions. From this work, the importance of solvation in stabilizing the metastable state is evident, as is the relationship between solution coordination and the ultimate crystal packing.

To increase our detailed understanding of these structural aspects of the nucleation process and the nature of the supersaturated metastable state, we now report the results of a further study using combined neutron scattering experiments

(with isotope substitution) and Monte Carlo-based empirical potential structure refinement (EPSR)^{11,12} to give a model structure consistent with measured scattering data. In this instance, our attention is focused on the simple aromatic carboxylic acid, benzoic acid (Figure 1). The carboxylic acid functionality is ubiquitous in organic solid state chemistry, and the balance of polar versus nonpolar aromatic character of this molecule is an important generic feature of many pharmaceutical and fine chemicals products. Its packing and H-bonding behavior in the solid state as well as its solution chemistry have been the subject of significant previous study.

In the crystalline state, carboxylic acids adopt one of two H-bonding motifs: the centric dimer or the chainlike catemer.¹³ Benzoic acid¹⁴ adopts the R₂²(8) dimer motif seen in Figure 1c (CSD Refcode BENZAC02, and visualized using Mercury¹⁵). Its known solution chemistry pre-1945, based on thermodynamic data, was summarized by Pauling in his book, *The Nature of the Chemical Bond*:¹⁶ “benzoic acid and other carboxylic acids have been shown to associate to double molecules in solution in certain solvents such as benzene, chloroform, carbon tetrachloride and carbon disulfide. Benzoic acid exists in monomeric form in solution in acetone, acetic acid, ethyl ether, ethyl acetate and phenol; in these solutions single molecules are stabilized by hydrogen bond formation with the solvent.” More recent studies on benzoic acid-methanol solutions by Tanevska-Osinska and Mishchenko^{17,18} using vapor pressure and heat of solution data indicate that, for concentrations up to 4.0 M and temperatures from 15 to 40 °C, the solutions obey Raoult’s law and are, essentially, ideal. These authors suggested that benzoic acid is present in solution as monomers which form hydrogen bonded complexes with methanol. This conclusion is also implied by Novak et al.¹⁹ through the use of NMR and FTIR measurements of 0.4 M solutions of benzoic acid in methanol together with semiempirical calculations, suggesting a 1:1 complex between benzoic acid and methanol.

In this current work, methanol solutions have been chosen for further study for two reasons: first, methanol offers reasonable solubility to benzoic acid (0.1632 mol fraction of benzoic acid in methanol at 25 °C,²⁰ as compared to 0.0005 in water); and second, the liquid structure of methanol has already been

* Corresponding author. E-mail: roger.davey@manchester.ac.uk.

[†] The University of Manchester.

[‡] University College London.

[§] ISIS Facility, STFC.

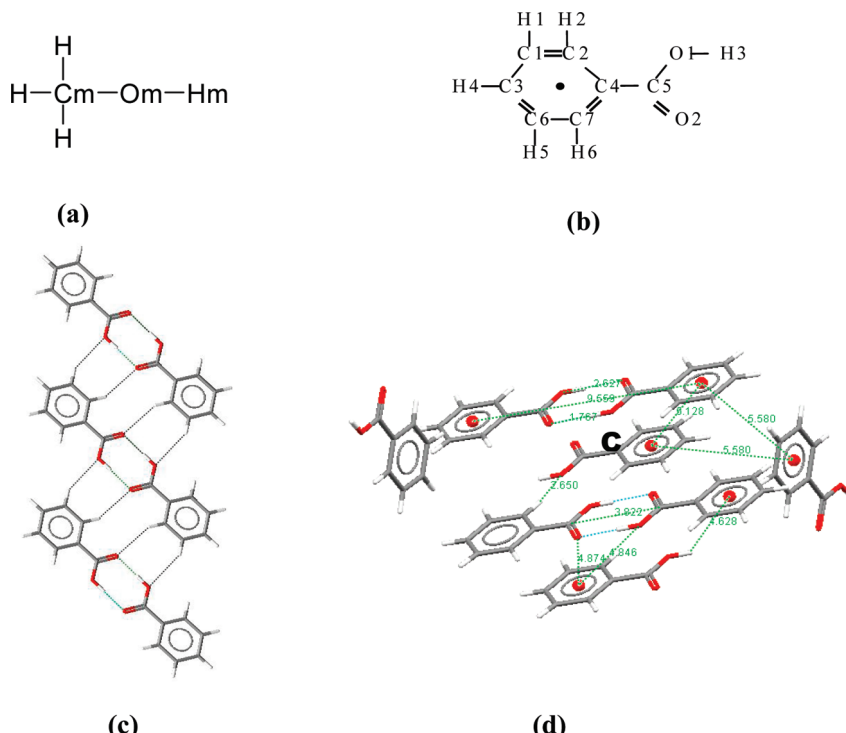


Figure 1. Methanol and benzoic acid. (a) methanol labeling used in EPSR simulation, (b) benzoic acid labeling used in EPSR simulation, (c) the dimer motif in benzoic acid crystals, and (d) the local environment of a central benzoic acid molecule (C) within its crystal structure.

studied using neutron scattering techniques^{21–23} and is one of the simplest molecules to model using EPSR.

Experimental Section

To perform scattering experiments giving appropriate contrast to interactions of interest and, hence, to extract structural data, it is necessary to use isotopically substituted samples.²⁴ Hence, C_6D_5COOD , C_6H_5COOD , and C_6H_5COOH , together with CH_3OH and CD_3OD , were used (all chemicals were purchased from Cambridge Isotope Laboratories) to prepare the following solutions: C_6H_5COOD in CD_3OD , C_6D_5COOD in CD_3OD , 1:1 C_6H_5COOD/C_6D_5COOD in CD_3OD ; C_6H_5COOH in CH_3OH , and 1:1 C_6H_5COOH/C_6D_5COOD in 1:1 CH_3OH/CD_3OD . Five distinct isotopically substituted solutions were thus required at each composition. Routinely, these would be supplemented by two further samples using C_6D_5COOH in CH_3OH ; however, due to the very low solubility of this pair (0.02 as compared with 0.16 mol fraction for C_6H_5COOH in CH_3OH), these experiments were not possible. At 15 °C, the 1:1 mixture of C_6H_5COOH/C_6D_5COOD in 1:1 CH_3OH/CD_3OD leaked, reducing the experimental data at this temperature to four data sets. Data was collected on a 0.1 and 0.16 (saturated) mole fraction of benzoic acid solution at 25 °C and, in addition, on the 0.16 mol fraction solution at 15 °C, where it would be supersaturated. The solubility at 15 °C is 0.142 mol fraction so that the supersaturation imposed ($\ln x_{25}/x_{15}$) was 0.12. The induction time for crystallization measured in an unstirred 25 mL vessel suggested that this solution should remain crystal-free for ~200 h, which is acceptable for the neutron-scattering experiments.

The densities of methanolic benzoic acid solutions having the compositions used in the experiments were measured (Anton Paar Density Meter) to be $0.8800 \times 10^3 \text{ kg m}^{-3}$ at 0.1 mol fraction and 25 °C, and for 0.16 mol fraction, 0.9023×10^3 and $0.9033 \times 10^3 \text{ kg m}^{-3}$ at 25 and 15 °C, respectively.

The experiments were performed using the Small Angle Neutron Diffractometer for Amorphous and Liquid Samples

(SANDALS) at the ISIS pulsed neutron source at the Rutherford Appleton Laboratory, U.K. Data were collected from samples contained in a titanium–zirconium alloy sample cell in periods of 6 h/sample. This type of cell gives a negligible coherent scattering contribution to the measured signal and has internal dimensions of 1 mm × 35 mm × 35 mm so that ~1.5 mL of solution was used in each cell. The cell was mounted in a holder, the temperature of which was controlled to a stability of ±0.1 °C using a circulating water bath.

Data were collected over scattering angles (2θ) between 3° and 40° and analyzed using the Gudrun routines²⁵ for neutron wavelengths in the range, $\lambda = 0.05–4.95 \text{ \AA}$. From these data, the total interference differential cross sections, $F(Q)$, (in which Q is the scattering vector, $Q = 4\pi/(\lambda \sin \theta)$), were generated.

Data Analysis

EPSR^{11,12,26} was used to build three-dimensional atomistic structural models, corresponding to the chosen compositions and temperatures and consistent with the measured neutron scattering data obtained from the solutions studied. Briefly, a reference set of atomic interaction potentials (defined by Lennard-Jones parameters and Coulomb charges)²⁷ are used to run a standard Monte Carlo simulation of a liquid. Once this simulation has reached equilibrium, the difference between the experimental and calculated neutron scattering structure factors is used to define a difference function and, hence, a series of perturbation potentials that are combined with the reference potentials to continue the Monte Carlo algorithm. Periodically, these perturbation functions are re-evaluated, and ultimately, this procedure generates a set of perturbation potentials that combine with the initial reference set to produce structural configurations within the simulation that agree with the experimental data used to drive the refinement.²⁶ At this point, the Monte Carlo simulation is continued and ensemble-average information is accumulated on the structural configurations of the atoms and molecules in the standard way. The combination of geometrical

TABLE 1: Benzoic Acid Bond Lengths and Angles Used during the EPSR Simulations to Constrain the Molecular Geometry²⁸

bond lengths/Å		bond angles/°	
C–C	1.40	O2–C5–O1	120
C4–C5	1.48	O1–C5–C4	120
C5–O1	1.36	O2–C5–C5	121
C5–O2	1.24	C–C–C	120
O1–H3	0.906	C–C–H	120
C–H	1.08	H3–O1–C5	109

TABLE 2: Bond Lengths and Angles for Methanol Used in the Simulations^{29,30}

bond lengths		bond angles	
Cm–H	1.080	H–Cm–H	109.470
Om–Hm	1.000	Cm–Om–Hm	109.470
Cm–Om	1.430	H–Cm–Om	109.470

TABLE 3: Lennard-Jones Parameters and Charges Used for the Atoms in Benzoic Acid³¹

atom	Lennard-Jones well depth/kJ mol ⁻¹	core diameter/Å	Coulomb charge
C1 (= C2 = C3 = C6 = C7)	0.293	3.550	-0.115
C4	0.293	3.550	0.000
C5	0.439	3.750	0.520
O1	0.711	3.000	-0.530
O2	0.879	2.960	-0.440
H1 (= H2 = H4 = H5 = H6)	0.000	0.000	0.115
H3	0.000	0.000	0.450

TABLE 4: Lennard-Jones Parameters and Effective Charges for Methanol³¹

atom	Lennard-Jones well depth/kJ mol ⁻¹	core diameter/Å	Coulomb charge
Cm	0.2760	3.5000	0.1450
Om	0.7110	3.0830	-0.6830
H	0.0126	1.8000	0.0400
Hm	0.0000	0.0000	0.4180

and density constraints imposed by the simulation restrict the range of the experimental results in a physically and chemically consistent set of structural solutions. This is the primary advantage of the EPSR method for the interpretation of experimental scattering data over more conventional direct analysis approaches.

Within these simulations, the average molecular geometry of the mixture constituents were constrained to the bond lengths and angles of Table 1 for benzoic acid and Table 2 for methanol. (For atom labeling, see Figure 1a and b.)

Tables 3 and 4 give the Lennard-Jones parameters and effective charges used in EPSR, for benzoic acid, and for methanol taken from Jorgensen et al.³¹ The instantaneous molecular geometries of the mixture components were periodically randomized within a simple harmonic potential model that aimed to capture the unavoidable quantum mechanical zero point disorder.³² At each concentration, simulations were run for the five isotopic compositions using the parameters and molecular structure in Tables 1–4. This combination of parameters and molecular structure was also chosen as the experimental data are very weakly weighted to the O_m...O_m correlation between the methanol molecules. The isotopic substitutions used to highlight methanol are focused on the methyl hydrogen sites, and the only constraint on the O_m...O_m correlation is through the well-defined molecular shape. This, however, prevents the EPSR simulation from arbitrarily refining this specific correlation. Thus, although the potential set chosen³¹ gave the most

reasonable distance between adjacent methanol oxygen atoms, conclusions involving the alcohol–alcohol hydrogen bonding will be weighted more heavily by the reference potential and geometric constraints used in the refinement than by the neutron scattering data.

Simulations (EPSRshell) were run on cubic boxes containing 30 benzoic acid and 270 methanol molecules of side length of 28.54 Å and an atomic density of 0.089 076 0 atoms Å⁻³; 48 benzoic acid and 252 methanol molecules of side length 29.27 Å and atomic density of 0.089 019 6 atoms Å⁻³; 48 benzoic acid and 252 methanol molecules of side length 29.16 Å and atomic density of 0.089 984 0 atoms Å⁻³ for 0.10 mol fraction at 25 °C, 0.16 mol fraction at 25 °C and 0.16 mol fraction at 15 °C, respectively. In each simulation, initial equilibration to the reference potentials was achieved after ~10⁵ atomic and molecular moves; the empirical potential evolved over around 10⁶ moves; and then finally, ensemble accumulations were gained over 10⁷ atomic and molecular moves. In each Monte Carlo cycle, every atom, molecule, and rotational group in the simulation is moved once.

Results and Discussion

Fits to the neutron scattering data for the 0.10 and 0.16 mol fraction solutions at 25 °C, and 0.16 mol fraction solution at 15 °C generated using EPSR are shown as interference cross sections and composite radial distribution functions in Figure 2. Although the fit to the data is good for all data sets, in some cases, there are deviations between the measured data and the EPSR fit below $Q < 2.5$ Å. These discrepancies, due to inelastic and self-scattering, do not make any difference to the correlations at the relevant intermolecular length scales^{33,34} and have been fully discussed previously.³⁵

An Overview of Solution Structure. A detailed discussion of the structures of the solutions necessitates access to selected partial radial distribution functions (pdfs; $g_{\alpha\beta}(r)$, the correlations between atoms of type α on one molecule and atoms of type β on other molecules), of which there are 190 for the benzoic acid–methanol system. Here, the number of these pdfs examined is restricted, first to those relating the “molecular centers” and, second, to those with the potential to yield insight into intermolecular hydrogen bonding. The former offer a useful overview of the solution structure and provide information on ring...ring interactions. Using the atomic numbering as before, (Figure 1), they describe the various correlations between the carboxyl carbon, C₅; the center of the phenyl ring (the black dot in Figure 1b); the methanol oxygen, O_m; and the methanol carbon, C_m. The related coordination numbers and associated interatomic distance ranges for these functions for the 0.10 mol fraction and 0.16 mol fraction solutions at 25 °C and the 0.16 mol fraction solutions at 25 and 15 °C are given in Tables 5 and 6; the associated pdfs themselves are provided in the Supporting Information (Figures S1 and S2). An instructive means of visualizing these data is via the spatial density functions (SDFs)^{36–38} which are three-dimensional maps showing the regions of space around a central atom or defined point on a molecule most likely to be occupied by the molecular centers or specific atoms of neighboring molecules.

These are seen in Figures 3–6 for the interactions discussed above with, for each figure, the solution concentration increasing from a to b with c supersaturated. Figure 3, relating to the –ring...C_m– contacts, thus offers a general impression of the solvation of benzoic acid by methanol, encompassing both the nonpolar interactions between the methyl group of the solvent and the aromatic ring as well as polar contacts with the

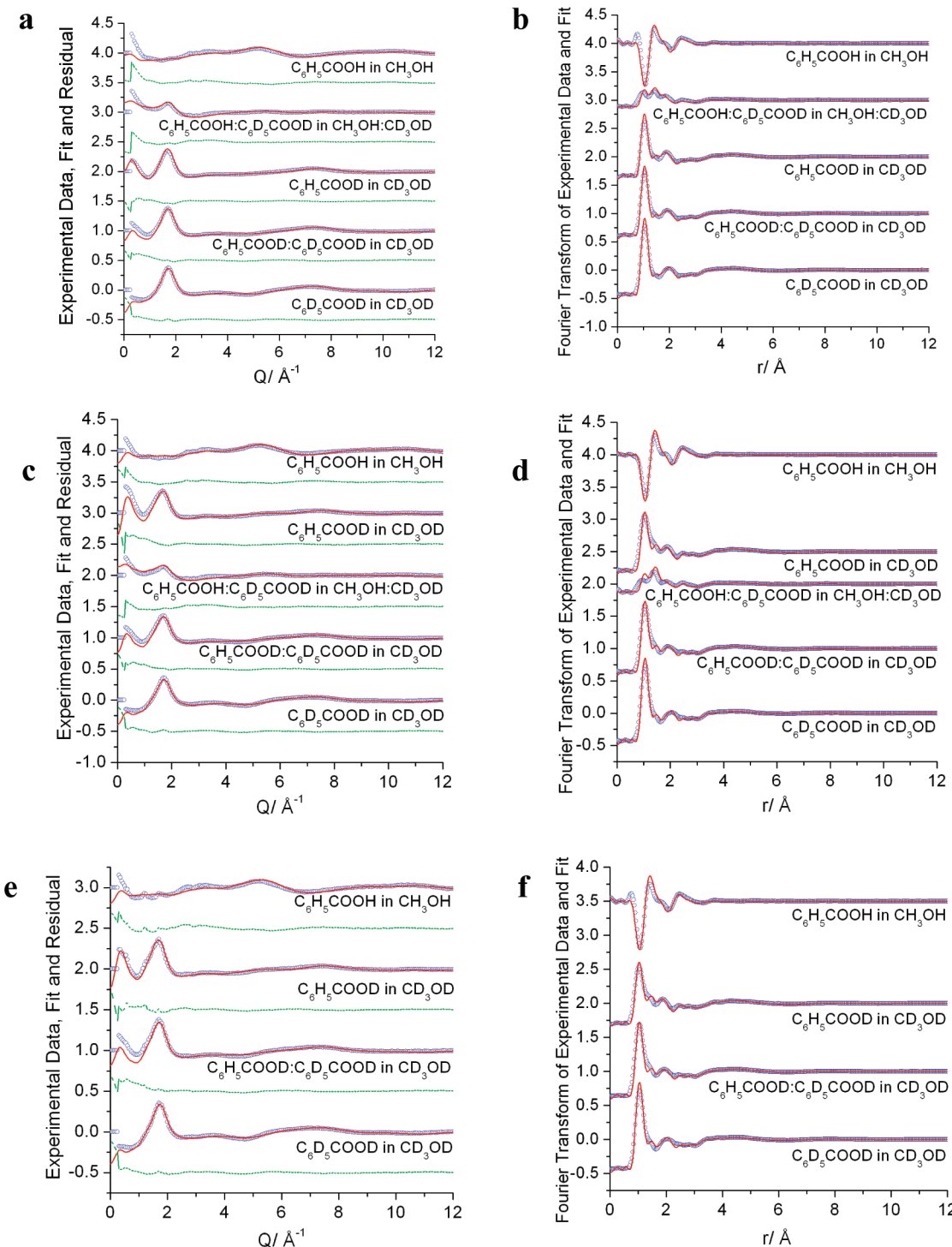


Figure 2. (Left) Experimentally measured $F(Q)$'s (blue circles), EPSR fits (red lines), and fit residuals (green dotted lines). (Right) Composite $g(r)$'s determined by Fourier transform of the experimental $F(Q)$'s (blue circles) and EPSR fits (red lines). Graphs have been offset for clarity. (a, b) 0.10 mol fraction of benzoic acid in methanol at 25 °C, (c, d) 0.16 mol fraction of benzoic acid in methanol at 25 °C, and (e, f) 0.16 mol fraction of benzoic acid in methanol at 15 °C.

carboxylic acid group. The former evidently favor the face of the phenyl ring, and the similarity between under- and supersaturated solutions is evident. The latter, seen in more detail in the $-C_5 \cdots O_m$ SDF of Figure 4, shows the H-bonding of methanol to the carboxylic acid group, with solvation of the hydroxyl group (large yellow lobe in the background of Figure 4) evidently unchanged with increasing concentration. At the same time, the carbonyl group (foreground of Figure 4) experiences increasing solvation from undersaturated through saturated to supersaturated solutions.

The benzoic acid–benzoic acid interactions are visualized in Figures 5 and 6 through the $-C_5 \cdots C_5-$ and ring \cdots ring SDFs. Figure 5 implies the absence of cyclic dimers in these solutions because these would be indicated by lobes underneath the C5 atom of the central benzoic acid molecule. The equivalence of under and supersaturation are again clear in this SDF: increasing concentration constrains the positions around the carbonyl group, whereas supersaturation expands them again. In terms of the ring–ring contacts, the similarity between the three solutions is apparent with the first shell contacts (3–5.5

TABLE 5: Coordination Numbers Calculated from Integration of the Molecular Centers' Functions and Partial Distribution Functions for 0.16 and 0.10 mol Fraction of Benzoic Acid in Methanol Solutions at 25 °C Using the Atomic Density and Limits Indicated in the Table^a

correlation	$R_{\min}/\text{\AA}$	$R_{\max}/\text{\AA}$	atomic density $\rho/\text{atom \AA}^{-3}$	0.16 methanolic benzoic acid, 25 °C coordination number (atoms)	atomic density $\rho/\text{atom \AA}^{-3}$	0.10 methanolic benzoic acid, 25 °C coordination number (atoms)		
C5–Om	2.50	4.20	0.01005	2.0	±0.2	0.01162	2.1	±0.3
	2.50	6.25		8.7	±0.4		8.9	±0.4
ring–ring	3.00	5.50	0.00191	0.8	±0.2	0.00129	0.7	±0.2
	3.00	7.10		2.5	±0.3		2.1	±0.4
C5–C5	3.00	5.00	0.00191	0.6	±0.1	0.00129	0.5	±0.2
	3.00	9.30		6.1	±0.5		4.5	±0.5
Ring–Cm	3.00	6.25	0.01005	9.2	±0.4	0.01162	10.1	±0.6
Om–Om	2.00	3.40	0.01005	1.7	±0.1	0.01162	1.8	±0.1
	2.00	5.90		8.7	±0.3		9.9	±0.3
O2–Hm	1.00	2.60	0.01005	0.6	±0.1	0.01162	0.7	±0.1
	1.00	5.90		7.3	±0.4		7.8	±0.5
H3–Om	1.00	2.50	0.01005	0.9	±0.1	0.01162	0.9	±0.2
	1.00	6.00		7.8	±0.4		8.5	±0.5
O1–O2	2.25	3.15	0.00191	0.1	±0.1	0.00129	0.1	±0.1
	3.15	5.60		0.8	±0.1		0.6	±0.1
H3–O2	2.25	5.60		0.9	±0.1		0.7	±0.2
	1.25	2.55	0.00191	0.1	±0.04	0.00129	0.1	±0.1
O1–Hm	1.25	4.70		0.5	±0.1		0.4	±0.1
	1.25	2.40	0.01005	0.2	±0.1	0.01162	0.2	±0.1
O1–Hm	2.40	4.25		2.0	±0.2		2.4	±0.3
	1.25	6.25		8.9	±0.4		9.6	±0.6
H2–O2	1.50	3.90	0.00191	0.3	±0.1	0.00129	0.3	±0.1
	1.50	8.00		3.6	±0.3		2.7	±0.3
O1–Om	2.25	3.20	0.01005	1.1	±0.1	0.01162	1.1	±0.2
	2.25	5.60		6.2	±0.4		6.6	±0.5
O2–H6	1.50	4.00	0.00191	0.3	±0.1	0.00129	0.2	±0.1
	1.50	8.00		3.6	±0.3		2.7	±0.3
O2–Om	2.25	3.25	0.01005	0.6	±0.1	0.01162	0.7	±0.2

^a Atom labels are described in Figure 1.

TABLE 6: Coordination Numbers Calculated from Integration of the Molecular Centers' Functions and Partial Distribution Functions for 0.16 mol Fraction of Benzoic Acid in Methanol Solutions at 25°C and 15°C Using the Atomic Density and Limits Indicated in the Table

correlation	$R_{\min}/\text{\AA}$	$R_{\max}/\text{\AA}$	atomic density $\rho/\text{atom \AA}^{-3}$	0.16 methanolic benzoic acid, 25 °C coordination number (atoms)	atomic density $\rho/\text{atom \AA}^{-3}$	0.16 methanolic benzoic acid, 15 °C coordination number (atoms)		
C5–Om	2.50	4.20	0.01005	2.0	±0.2	0.01016	2.1	±0.2
	2.50	6.25		8.7	±0.4		8.9	±0.4
ring–ring	3.00	5.50	0.00191	0.8	±0.2	0.00194	0.8	±0.2
	5.50	7.10		1.7	±0.3		1.8	±0.3
C5–C5	3.00	5.00	0.00191	0.6	±0.1	0.00194	0.5	±0.1
	3.00	9.30		6.1	±0.5		6.1	±0.5
ring–Cm	3.00	6.25	0.01005	9.2	±0.4	0.01016	9.4	±0.4
Om–Om	2.00	3.40	0.01005	1.7	±0.1	0.01016	1.7	±0.1
	2.00	5.90		8.7	±0.3		8.9	±0.3
O2–Hm	1.00	2.60	0.01005	0.6	±0.1	0.01016	0.7	±0.1
	1.00	5.90		7.3	±0.4		7.4	±0.4
H3–Om	1.00	2.50	0.01005	0.9	±0.1	0.01016	0.9	±0.1
	1.00	6.00		7.8	±0.4		8.0	±0.4
O1–O2	2.25	3.55	0.00191	0.1	±0.05	0.00194	0.1	±0.04
	2.25	5.60		0.9	±0.1		0.9	±0.1
H3–O2	1.25	2.55	0.00191	0.1	±0.04	0.00194	0.1	±0.04
	1.25	4.70		0.5	±0.1		0.5	±0.1
O1–Hm	1.25	2.40	0.01005	0.2	±0.1	0.01016	0.2	±0.1
	2.40	4.25		2.0	±0.2		2.4	±0.2
O1–Hm	1.25	6.25		8.9	±0.4		9.1	±0.4
	1.50	3.75	0.00191	0.3	±0.1	0.00194	0.2	±0.1
H2–O2	1.50	8.00		3.6	±0.3		3.6	±0.3
	2.25	5.60	0.01005	1.1	±0.1	0.01016	1.1	±0.1
O2–H6	1.50	3.75	0.00191	0.2	±0.1	0.00194	0.3	±0.1
	1.50	8.00		3.6	±0.3		3.6	±0.3

Å), implied in Figure 6, via face-to-face, π – π interactions and the second shell interactions (5.5–7.1 Å) involving face-to-edge contacts around the top of the benzene ring and the carboxylic acid groups. It is notable that in the supersaturated solution, these latter contacts appear to be closer than in the saturated solution. The face–edge interactions in the 0.10 mol fraction of benzoic acid solution at 25 °C appear less disordered and

more orientationally defined than the same interaction in the saturated and supersaturated solutions.

Thus, in examining the benzoic acid–methanol and benzoic acid–benzoic acid contacts through the SDFs, it is evident that when placing the solution into the supersaturated state, the three-dimensional structure of the liquid changes to adopt local correlations reflecting the structure of an unsaturated solution

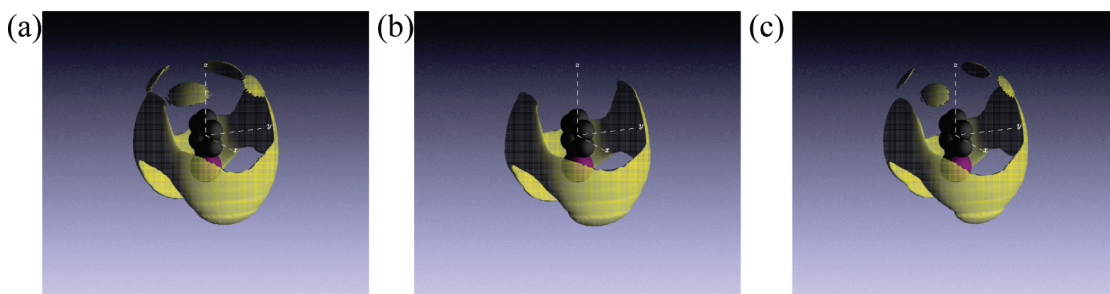


Figure 3. SDFs for the $-ring \cdots Cm-$ interactions with the phenyl ring at the center and the yellow lobes indicate the most likely sites occupied by the methanol carbon atoms. The phenyl ring is indicated by six dark gray spheres attached to a purple sphere, which is not shown as individual atoms, because this group is free to rotate. SDFs for (a) 0.1 mol fraction benzoic acid in methanol solution at 25 °C, (b) 0.16 mol fraction benzoic acid in methanol solution at 25 °C, and (c) 0.16 mol fraction of benzoic acid in methanol solution at 15 °C. The isosurface level used is 10% in the distance range 3–6.25 Å.

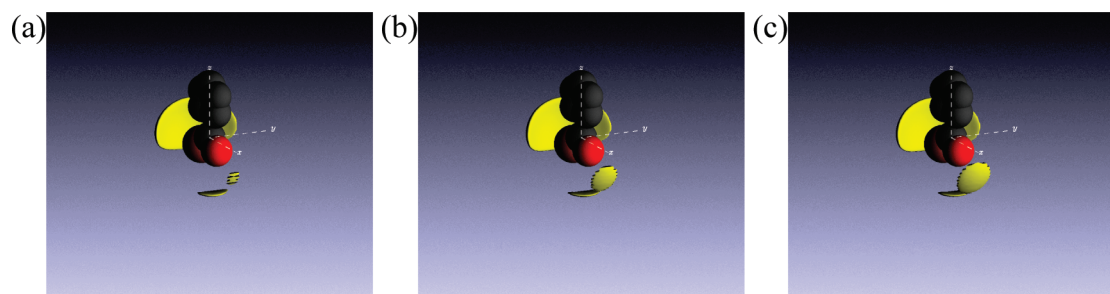


Figure 4. SDFs for the $-C5 \cdots Om-$ interactions with the benzoic acid C5 atom at the center. The yellow lobes indicate the most likely sites occupied by the methanol oxygen atoms. The C5 atom is the dark gray sphere at the center attached to both a phenyl ring and a red sphere, which is the carbonyl oxygen, and to a slightly larger sphere that lies toward the back of the molecule, which is the hydroxyl group. SDFs for (a) 0.1 mol fraction benzoic acid in methanol solution at 25 °C, (b) 0.16 mol fraction benzoic acid in methanol solution at 25 °C, and (c) 0.16 mol fraction benzoic acid in methanol solution at 15 °C. The isosurface level used is 25% in the distance range 2.5–4.2 Å.

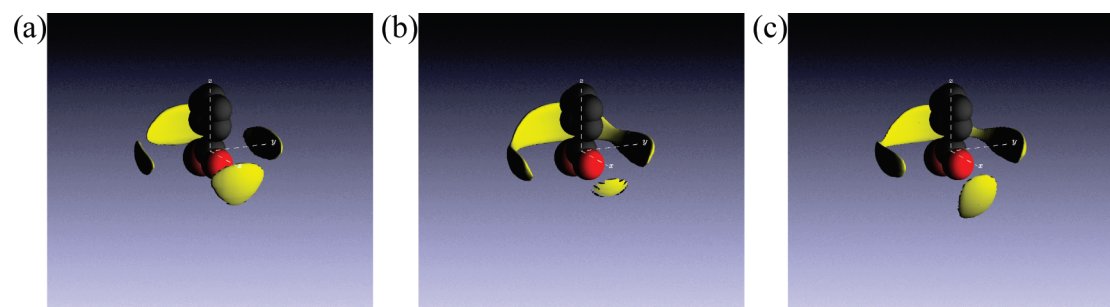


Figure 5. Spatial density functions for the $-C5 \cdots C5-$ interactions with the benzoic acid C5 atom at the center of the central and neighboring molecules. SDFs shown for (a) 0.1 mol fraction benzoic acid in methanol solution at 25 °C, (b) 0.16 mol fraction benzoic acid in methanol solution at 25 °C, and (c) 0.16 mol fraction benzoic acid in methanol solution at 15 °C. The isosurface level used for all the SDFs is 10% in the distance range 3–5.15 Å.

rather than a saturated solution. This enhanced solvation mirrors the result found in aqueous urea and again suggests the role of solvation as a means of stabilizing the supersaturated state. At the same time, however, supersaturation does appear to compress the ring–ring interactions, hence, packing the benzoic acid molecules closer together. This balance of enhanced solvation with increased packing could well be an essential step along the route to crystallization.

A quantitative perspective of these trends can be gleaned from Tables 5 and 6, which show that, as expected, upon dilution, there are increasing numbers of $-C5 \cdots Om-$ and ring $\cdots Cm-$ contacts and decreasing numbers of ring–ring and $-C5 \cdots C5-$ interactions. As far as the carboxylic acid group is concerned, the $-C5 \cdots Om-$ pdf shows (see Supporting Information Figure S1 and Table 5) that each benzoic acid molecule is coordinated, probably hydrogen bonded, to two methanol molecules. For benzoic acid–benzoic acid interactions, in both saturated and undersaturated solutions, the coordination of the $-C5 \cdots C5-$

interaction is about 0.5 in the distance range 3–5 Å (peaking at 4.4 Å), which could imply hydrogen bonding between benzoic acid molecules.

The ring \cdots ring pdf that peaks at 5.50 Å (Supporting Information Figure S1) suggests that a central benzoic acid molecule is coordinated, on average, to two and 2.5 other benzoic acid molecules (out to 7.1 Å) in the undersaturated and saturated solutions, respectively. If these $-C5 \cdots C5-$ and ring \cdots ring contacts were associated with hydrogen bonded cyclic dimers equivalent to those in the crystal structure, then the corresponding $-C5 \cdots C5-$ and ring–ring distances might be expected to be close to the solid state values of 3.8 and 9.6 Å. Instead, they are significantly longer and shorter, respectively, peaking at 4.4 and 5.5 Å, respectively (Supporting Information Figure S1), and placing doubt on the existence of H-bonded dimers in these solutions, a point discussed in more detail later. It is clear that upon supersaturation, the $-C5 \cdots C5-$ interaction

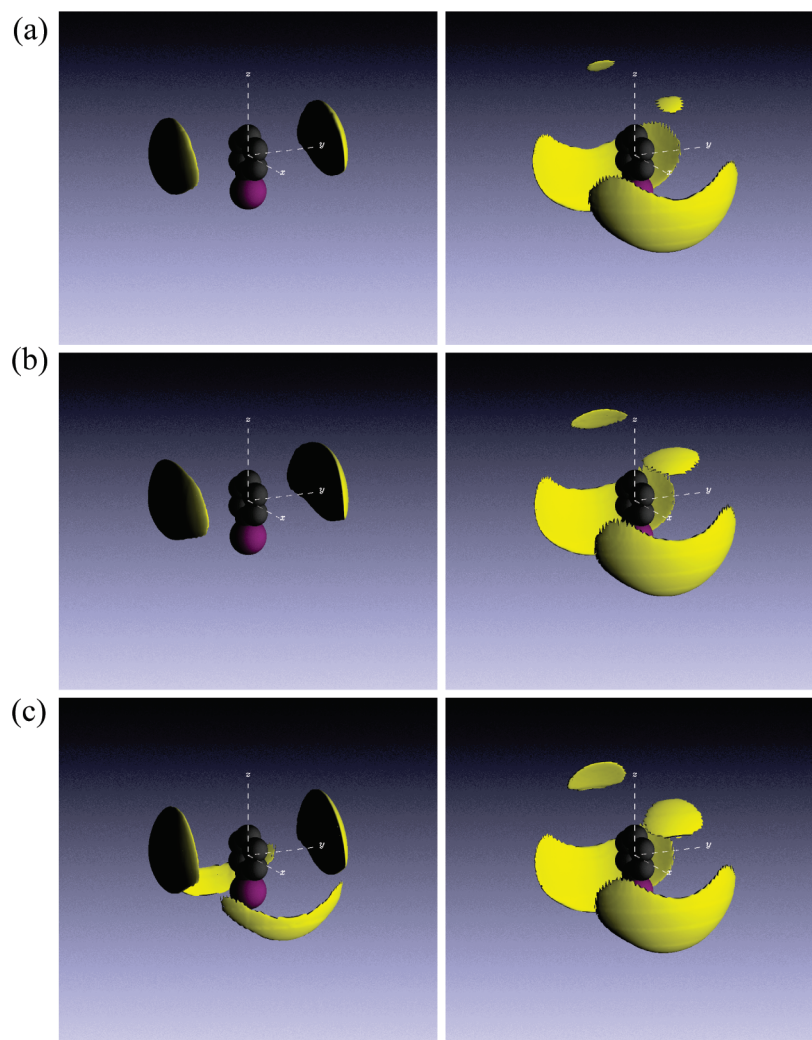


Figure 6. SDFs for the $-ring \cdots ring-$ interactions. For the central molecule, the phenyl ring is shown by six gray spheres. The carboxylic group is shown as a purple sphere at the bottom of the benzoic acid molecule because this group is free to rotate. (Top) SDFs for 0.1 mol fraction benzoic acid in methanol solution at 25 °C, (middle) 0.16 mol fraction benzoic acid in methanol solution at 25 °C, and (bottom) 0.16 mol fraction benzoic acid in methanol solution at 15 °C. The isosurface level used for all the SDFs is 5% in the distance ranges (left) 3–5.5 Å and (right) 5.5–7.1 Å.

decreases and the $ring \cdots ring$ interaction increases slightly, but there are no obvious differences in the other molecular centers' functions.

Upon supersaturation (Table 6 and Figure S2), the coordination of both the $-C_5 \cdots O_m-$ and $ring \cdots ring$ interactions increases slightly. The number of $-C_5 \cdots C_5-$ contacts decrease from 0.6 in the saturated solution to 0.5 in the supersaturated solution. Hence, it would appear that upon supersaturation, the benzoic acid polar group becomes more solvated with a simultaneous increase in the hydrophobic $ring \cdots ring$ interactions, exactly the conclusion visualized in the SDF (see Figures 4 and 6).

The methanol–methanol coordination revealed in the $-O_m \cdots O_m$ $g(r)$ increases from 1.7 to 1.8 upon dilution in the distance range 2–3.4 Å and implies the existence of hydrogen bonded methanol trimers in both solutions. These numbers compare very favorably with the coordination of 1.8 for pure methanol at 25 °C calculated using neutron scattering and EPSR:³⁹ 1.8 at 20 °C⁴⁰ and 1.7 at 20 °C,⁴¹ both determined by X-ray diffraction, supporting the near ideality of these solutions discussed above. The corresponding SDFs are shown in the Supporting Information, Figure S3.

Partial Radial Distribution Functions. To explore in further detail the specific (H-bonded) intermolecular interactions in-

ferred from the molecular centers' data above, the relevant partial radial distribution functions are shown in Figure 7. Integration over the first peaks in these pdfs (graphical data for the 0.16 mol fraction solution at 25 and 15 °C are shown in the main text, Figure 7; the 0.1 and 0.16 mol fraction at 25 °C may be found in Supporting Information Figure S4) shows that each carboxylic acid group is H-bonded to methanol via three interactions described by the $-O_2 \cdots H_m-$, $-H_3 \cdots O_m-$, and $-O_1 \cdots H_m$ correlations, providing a total hydrogen bonded coordination of 1.7 (Table 5). This increases to 1.8 (Table 6) upon supersaturation through a slightly increased solvation of the carbonyl group, as inferred above from the molecular centers. There is, in addition, one H-bond, $-H_3 \cdots O_2-$, between neighboring carboxylic acid groups with a coordination of 0.1 that is unchanged with concentration. The associated oxygen–oxygen contacts ($-O_2 \cdots O_m$, $O_1 \cdots O_m$ and $-O_1 \cdots O_2$) are consistent with this interpretation, as seen in Tables 5 and 6. It is clear that the overwhelming contribution (1.1 vs 0.6) to the solvation of the acid group is through the hydroxyl–hydroxyl contacts, precisely as revealed in Figure 5.

It is noted that the second peak at 3.35 Å in the $-O_1 \cdots H_m$ correlations suggests the coordination of a second solvation shell of 2–2.4 methanol molecules that are not H-bonded. A similar second coordination peak is evidenced for $-O_2 \cdots H_m$ but

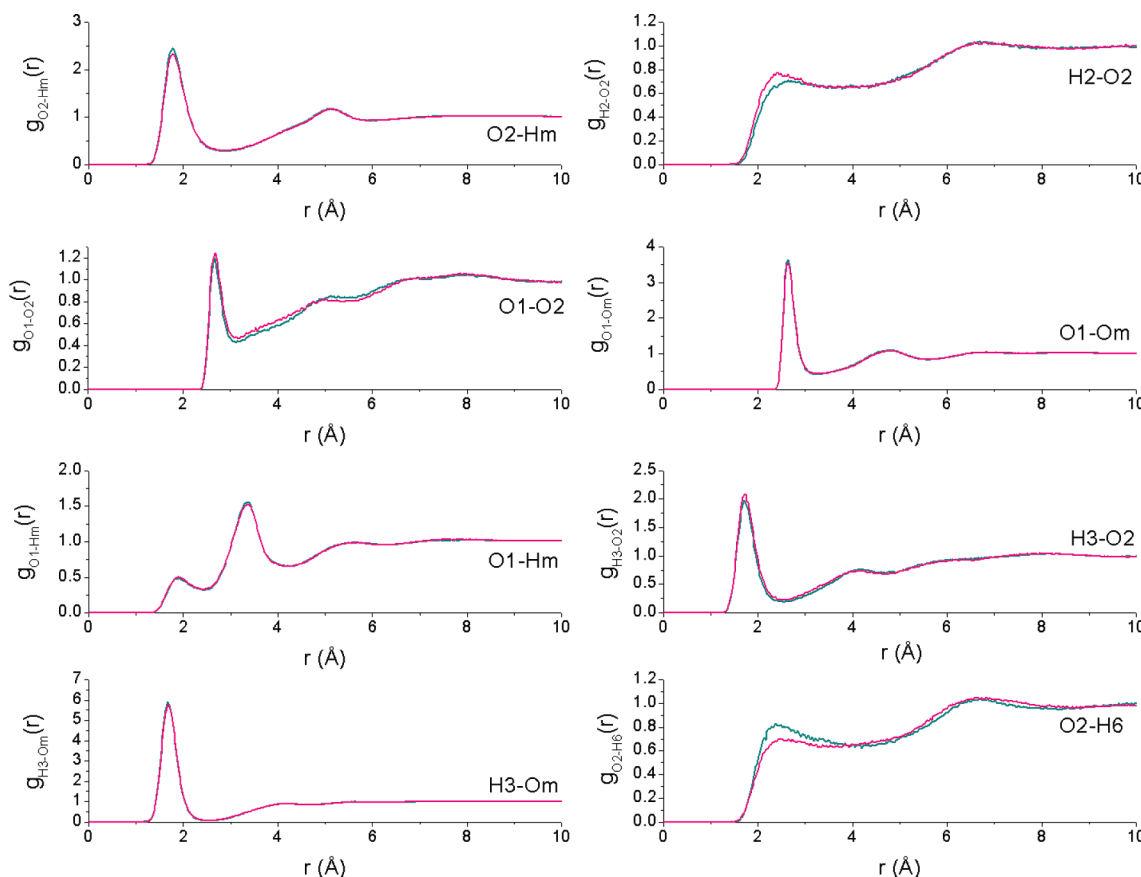


Figure 7. Partial radial distribution functions for 0.16 mol fraction of benzoic acid in methanol at 15 °C (blue) as compared with 0.16 mol fraction of benzoic acid in methanol at 25 °C (pink).

farther out at 5 Å and significantly less well-defined than for the hydroxyl group. The total benzoic acid–benzoic acid H-bonded contacts are evidently insensitive to concentration and comprise the nearest-neighbor coordination to the carbonyl oxygen ($-H_3\cdots O_2-$ as described above; coordination number 0.1; 1.74 Å) and the weaker $-C-H\cdots O-$ interactions through $-H_6\cdots O_2-$ and $-H_2\cdots O_2-$ contacts (0.6 in total, 2.5 Å). To our knowledge, although the existence of such short contacts is well-known in molecular crystals,⁴² this is the first time it has been confirmed in solutions. The $-O\cdots H-$ distance of 2.5 Å observed in these solutions compares well with 2.65 Å found in the crystal structure of benzoic acid and, as expected, is less than the sum of the oxygen and hydrogen van der Waals radii, 2.7 Å. The $-C_5\cdots C_5-$ coordinations of 0.5 in dilute and 0.6 in the saturated solution correlate well with these totals.

Taking the various solute–solute pdfs together, it is possible to consider whether there is a single molecular dimer, similar to that in the crystal structure (Figure 1d), that would account for all the observed contacts. It is evident that in the crystal, for a pair of molecules interacting through a face–edge contact, the ring–ring and $-C_5\cdots C_5-$ distances of 5.58 and 8.1 Å are a reasonable match to the solution values of 5.5 and 8.0 Å. This dimer, however, does not allow for the observed $-C_5\cdots C_5-$ peak seen in solution at 4.4 Å (Supporting Information Figures S1 and S2). Equally, a pair of molecules involved in a $-CH\cdots O-$ interaction in the crystal has $-C_5\cdots C_5-$ and ring–ring distances of 5.84 and 7.5 Å; these are not seen in the solutions.

As discussed above, the dimensions of the solution phase $-C_5\cdots C_5-$ and ring–ring contacts are also inconsistent with the existence of hydrogen bonded cyclic dimers, and indeed,

this conclusion is supported by the low $-H_3\cdots O_2-$ coordination number of 0.1. It would thus appear that, although there is evidence of H-bonded contacts between benzoic acid molecules, the cyclic H-bonded dimer is not a major feature of these solutions. Indeed, pursuant to this, in the crystal structures of other carboxylic acids that contain hydrogen bonded chains rather than dimers (e.g., tetrolic acid (ref code3 TETROL01), acetic acid (ACETAC01), and oxalic acid (OXALAC06)), the equivalent $-C_5\cdots C_5-$ contact occurs at longer distances than for the cyclic dimer –4.225, 4.196, and 4.415 Å, respectively, much closer to the $-C_5\cdots C_5-$ distance (4.4 Å) in the benzoic acid solutions investigated here. This suggests that the solute–solute hydrogen bonded interactions occurring in these solutions are closer in concept to a catemeric motif than a dimer.

Overall, therefore, it is concluded that the solute–solute interactions in these methanolic solutions are dominated by a combination of $\pi-\pi$ (ring–ring), face–edge, and $-C-H\cdots O-$ contacts. As far as the acid $-COOH$ group is concerned, its H-bonded interactions are clearly dominated by methanol solvation.

The SDFs of Figures 4–6 reveal that upon supersaturation, the benzoic acid polar group becomes more solvated, with a simultaneous increase in the hydrophobic ring–ring interactions. The nature of this increased solvation has now been linked specifically to the $-O_2\cdots Hm-$ pdf with the coordination number out to 2.6 Å, increasing from ~0.6 to ~0.7, reflecting the related change in contacts on going from a saturated to an undersaturated solution. In the second-nearest-neighbor coordination sphere, the $-O_1\cdots Hm-$ pdf peaks at 3.35 Å, and the coordination numbers increase on supersaturation from 2.0 to 2.4, again behavior that is identical to the observed dilution

effect evident from the data in Table 5. These data shed no further light on the nature of the enhanced ring–ring contacts in the supersaturated state except that they appear to occur at distances out to 7 Å.

Discussion

The data presented provide a picture in which each carboxylic acid group is solvated by approximately two methanol molecules (at a distance out to 4.2 Å) and interacts with one other carboxylic acid group (out to 5 Å). Thus, two methanol molecules are hydrogen bonded to the carbonyl and hydroxyl groups of the carboxylic acid, and the self-association appears to occur via an H-bond that is suggestive of a chain rather than dimer motif. It is clear that methanol is significantly more successful at hydrogen bonding to the carboxylic acid group than other benzoic acid molecules: the coordination of 1.7 for methanol compares to 0.1 for benzoic acid. This probably reflects the reduced level of steric hindrance due to the smaller size of the methanol molecule. Interestingly, a similar effect is found with alcohols in water: the water favors the alcohol OH, suppressing alcohol dimerization.³⁸ For the first time, in solutions we find evidence of weak –CH···O– hydrogen bonded interactions between the aromatic rings and the carboxylic acid groups on neighboring benzoic acid molecules as well as π–π (ring–ring) and face–edge contacts.

In the context of crystal nucleation from these solutions, each benzoic acid ring is surrounded by about nine methanol molecules out to 6.25 Å and about five other benzoic acid molecules up to 7.1 Å and three involved in π–π and face–edge contacts, and approximately two are involved in weak –C–H···O– interactions. In its crystal structure, for each central benzoic acid molecule (Figure 1d), there is one molecule held in the dimer, one molecule held in a face-to-edge interaction, two molecules held by weak –C–H···O– interactions, and two molecules held by π–π interactions. This makes a total of six nearest neighbors for each central benzoic acid molecule. Hence, in solution at a local level, there are enough benzoic acid molecules to satisfy the nearest-neighbor requirements of the crystal structure for all the required interactions apart from the dimer hydrogen bond, which does not appear to be present in these solutions. The enhanced solvation of the polar carboxyl group and concomitant increase in nonpolar contacts between benzoic acid molecules is reminiscent of micelle formation in surfactant solutions, and this may provide a useful picture of the nucleation process and an initial stabilization mechanism for cluster formation. Subsequently, of course, significant internal rearrangement is essential, with the desolvation of the carboxylic acid groups and creation of H-bonded dimers being a crucial feature of the transformation of a cluster to a supernucleus. Again, as with urea⁹ and hexamethylene tetramine,¹⁰ this study emphasizes the importance of desolvation in the crystallization pathway.

Conclusions

This work has demonstrated the application of combined neutron-scattering experiments and empirical potential structure refinement to the study of the supersaturated state. This approach offers detailed insights into the time-averaged environment of solvent and solute molecules and in this case has illustrated the roles of H-bonding and ring···ring interactions in determining the nature of the overall solvation and self-assembly of benzoic acid in methanol. The experimental time scale of this approach makes it unsuitable for exploring a detailed kinetic pathway

during nucleation itself; nevertheless, it does enable a comparison of supersaturated and crystalline environments of the solute molecules.

Acknowledgment. EPSRC and STFC are acknowledged for financial support.

Supporting Information Available: Additional information as noted in text. This material is available free of charge via the Internet at <http://pubs.acs.org>.

References and Notes

- Davey, R. J.; Garside, J. *From molecules to crystallizers—an introduction to crystallisation*; Oxford University Press: Oxford, 2000.
- Volmer, M. *Kinetic der Phasenbildung*; Steinkopf: Dresden, 1939.
- Allen, F. H. *Acta Crystallogr.* **2002**, *B58*, 380–388.
- Davey, R. J.; Allen, K.; Blagden, N.; Cross, W. I.; Lieberman, H. F.; Quayle, M. J.; Righini, S.; Seton, L.; Tiddy, G. J. T. *CrystEngComm* **2002**, *4*, 257–264.
- Spitaleri, A.; Hunter, C. A.; McCabe, J. F.; Packer, M. J.; Cockcroft, C. S. L. *CrystEngComm* **2004**, *6*, 489–493.
- Davey, R. J.; Mughal, R. G.; Parveen, S. *Cryst. Growth Des.* **2006**, *6*, 1788–1796.
- Chiarella, R. A.; Gillon, A. M.; Burton, R. C.; Davey, R. J.; Sadiq, G.; Auffret, A.; Cioffi, M.; Hunter, C. A. *Faraday Discuss.* **2007**, *136*, 179–193.
- Chadwick, K.; Davey, R. J.; Dent, G.; Pritchard, R. G.; Hunter, C. A.; Musumeci, D. *Cryst. Growth Des.* **2009**, *9*, 1990–1999.
- Burton, R. C.; Ferrari, E. S.; Davey, R. J.; Hopwood, J.; Quayle, M. J.; Finney, J. L.; Bowron, D. T. *Cryst. Growth Des.* **2008**, 1559–1565.
- Burton, R. C.; Ferrari, E. S.; Davey, R. J.; Finney, J. L.; Bowron, D. T. *J. Phys. Chem. B* **2009**, *113*, 5967–5977.
- Soper, A. K. *Chem. Phys.* **1996**, *202*, 295–306.
- Soper, A. K. *Mol. Phys.* **2001**, *99*, 1503–1516.
- Beyer, T.; Price, S. L. *J. Phys. Chem. B* **2000**, *104*, 2647–2655.
- Feld, R.; Lehmann, M. S.; Muir, K. W.; Speakman, J. C. Z. *Kristallogr.* **1981**, *157*, 215–231.
- Macrae, C. F.; Bruno, I. J.; Chisholm, J. A.; Edgington, P. R.; McCabe, P.; Pidcock, E.; Rodriguez-Monge, L.; Taylor, R.; van de Streek, J.; Wood, P. A. *J. Appl. Crystallogr.* **2008**, *41*, 466–470.
- Pauling, L. *The Nature of the Chemical Bond and the Structure of Molecules and Crystals: An Introduction to Modern Structural Chemistry*; Cornell University Press: Ithaca, NY, 1945; p 307.
- Tanewsk-Osinska, S.; Mishchenko, K. P. *Russ. J. Phys. Chem.* **1966**, *40*, 342–344.
- Tanewsk-Osinska, S.; Mishchenko, K. P. *Russ. J. Phys. Chem.* **1968**, *42*, 254–256.
- Novak, P.; Vikićtopic, D.; Meic, Z.; Sekusak, S.; Sabljic, A. J. *Mol. Struct.* **1995**, *356*, 131–141.
- Beerbower, A.; Wu, P. L.; Martin, A. J. *Pharm. Sci.* **1984**, *73*, 179–188.
- Yamaguchi, T.; Hidaka, K.; Soper, A. K. *Mol. Phys.* **1999**, *96*, 1159–1168.
- Dixit, S.; Crain, J.; Poon, W. C. K.; Finney, J. L.; Soper, A. K. *Nature* **2002**, *416*, 829–832.
- Soper, A. K.; Dougan, L.; Crain, J.; Finney, J. L. *J. Phys. Chem. B* **2006**, *110*, 3472–3476.
- Finney, J. L.; Soper, A. K. *Chem. Soc. Rev.* **1994**, *23*, 1–10.
- Bowron, D. T.; Finney, J. L.; Soper, A. K. *J. Am. Chem. Soc.* **2006**, *128*, 5119–5126.
- Soper, A. K. *Phys. Rev. B* **2005**, *72*, 104204-1–104204-12.
- Soper, A. K.; Castner, E. W.; Luzar, A. *Biophys. Chem.* **2003**, *105*, 649–666.
- Jorgensen, W. L.; Nguyen, T. B. *J. Comput. Chem.* **1993**, *14*, 195–205.
- Soper, A. K. Empirical Potential Structure Refinement - EPSRshell - "A User's Guide"; <http://www.isis.stfc.ac.uk/groups/disordered-materials/downloads/empirical-potential-structure-refinement6157.html> (accessed June 14, 2010).
- Ferrari, E. S.; Burton, R. C.; Davey, R. J.; Gavezzotti, A. *J. Comput. Chem.* **2006**, *27*, 1211–1219.
- Jorgensen, W. L.; Maxwell, D. S.; TiradoRives, J. *J. Am. Chem. Soc.* **1996**, *118*, 11225–11236.
- Soper, A. K. *Chem. Phys.* **2000**, *258*, 121–137.
- Bowron, D. T.; Moreno, S. D. *J. Chem. Phys.* **2002**, *117*, 3753–3762.
- Dixit, S.; Soper, A. K.; Finney, J. L.; Crain, J. *Europhys. Lett.* **2002**, *59*, 377–383.
- Soper, A. K.; Luzar, A. *J. Chem. Phys.* **1992**, *97*, 1320–1331.

- (36) Svishchev, I. M.; Kusalik, P. G. *J. Chem. Phys.* **1993**, *99*, 3049–1993.
- (37) Bowron, D. T.; Finney, J. L; Soper, A. K. *Mol. Phys.* **1998**, *93*, 531–543.
- (38) Bowron, D. T.; Finney, J. L.; Soper, A. K. *J. Phys. Chem. B* **1998**, *102*, 3551–3563.
- (39) Yamaguchi, T.; Hidaka, K.; Soper, A. K. *Mol. Phys.* **1999**, *97*, 603–605.
- (40) Narten, A. H.; Habenschuss, A. *J. Chem. Phys.* **1984**, *80*, 3387–3391.
- (41) Vahvaselka, K. S.; Serimaa, R.; Torkkeli, M. *J. Appl. Crystallogr.* **1995**, *28*, 189–195.
- (42) Desiraju, G. R.; Steiner, T. *The Weak Hydrogen Bond in Structural Chemistry and Biology*; Oxford University Press: New York, 1999.

JP103099J